Trade-offs constrain adaptive pathways to T6 survival

Kathryn A. MacGillivray[1,2,3,5], Siu Lung Ng[1,2,3,5], Sophia Wiesenfeld[1,2,3], Randi L. Guest[4], Tahrima Jubery[1,2,3], Thomas J. Silhavy[4], William C. Ratcliff*[1,2,3], Brian K. Hammer*[1,2,3]

[1]School of Biological Sciences, Georgia Institute of Technology, Atlanta, Georgia, USA

[2]Parker H. Petit Institute for Bioengineering & Bioscience, Georgia Institute of Technology, Atlanta, Georgia, USA

[3]Center for Microbial Dynamics and Infection, Georgia Institute of Technology, Atlanta, Georgia, USA

[4]Department of Molecular Biology, Princeton University, Princeton, New Jersey, USA

[5]indicates equal contributions

*Corresponding author:

william.ratcliff@biology.gatech.edu, brian.hammer@biology.gatech.edu

Classification: Evolution, Biological Sciences

Keywords: Experimental evolution, type VI secretion system, resistance, antagonism

Significance

Bacteria are the most abundant organisms on Earth and often live in dense, diverse communities, where they interact with each other. One of the most common interactions is antagonism. While most research has focused on diffusible toxins (e.g., antibiotics), bacteria have also evolved a contact-dependent nano-harpoon, the Type VI Secretion System (T6), to kill neighboring cells and compete for resources. While the co-evolutionary dynamics of antibiotic exposure is well understood, no prior work has examined how targets of T6 evolve resistance. Here, we use experimental evolution to observe how an *Escherichia coli* target evolves resistance to T6 when it is repeatedly competing with a *Vibrio cholerae* killer. After 30 rounds of competition, we identified mutations in three genes that improve *E. coli* survival, but found that these mutations come at a cost to other key fitness components. Our findings provide new insight into how contact-dependent antagonistic interaction drives evolution in a polymicrobial community.

Abstract

Many microbial communities are characterized by intense competition for nutrients and space. One way for an organism to gain control of these resources is by eliminating nearby competitors. The Type VI Secretion System (T6) is a nano-harpoon used by many bacteria to inject toxins into neighboring cells. While much is understood about mechanisms of T6-mediated toxicity, little is known about the ways that competitors can defend themselves against this attack, especially in the absence of their own T6. Here we use directed evolution to examine the evolution of T6 resistance, subjecting eight replicate populations of *Escherichia coli* to T6 attack by *Vibrio cholerae*. Over ~500 generations of competition, the *E. coli* evolved to survive T6 attack an average of 27-fold better than their ancestor. Whole genome sequencing reveals extensive parallel evolution. In fact, we found only two pathways to increased T6 survival: *apaH* was mutated in six of the eight replicate populations, while the other two populations each had mutations in both *yejM* and *yjeP*. Synthetic reconstruction of individual and combined mutations demonstrate

that *yejM* and *yjeP* are synergistic, with *yejM* requiring the mutation in *yejP* to provide a benefit. However, the mutations we identified are pleiotropic, reducing cellular growth rates, and increasing susceptibility to antibiotics and elevated pH. These trade-offs underlie the effectiveness of T6 as a bacterial weapon, and help us understand how the T6 shapes the evolution of bacterial interactions.

Introduction

Bacteria are one of the most common forms of life on Earth and often live in polymicrobial biofilms. Within this complex community, negative bacterial interactions are the norm[1], constantly competing for resources such as nutrients and space. One way for bacteria to gain an advantage over their competitors is by killing. They have developed two major classes of antagonistic mechanisms to eliminate competitors: diffusible and contact-dependent. Diffusible antibacterial molecules have been extensively described in soil bacteria like *Streptomyces*, which produces antibiotics (e.g. streptomycin, kanamycin, and tetracycline) to kill competitors, gain resources for their own population, and maintain symbiosis with associated plants[2]. *Pseudomonas aeruginosa* is also known to secrete lethal toxins like pyocyanin, exotoxin A, and ExoU that aid in competing against other microbes and human cells during infections[3–5]. On the other hand, contact-dependent antagonisms are less diverse and understudied in the social interaction aspects. The type VI secretion system (T6) discovered in 2006, for example, is a contact-dependent “nano-harpoon” similar to a contractile spear that kills neighboring cells by injecting them with a set of toxic proteins[6]. The T6 is estimated to be found in ~25% of all Gram-negative bacterial species[7], and targets diverse cell types, including eukaryotes like macrophages and largely Gram-negative bacteria like *Escherichia coli*, in both an environmental and host context[6,8].

While the regulation, genetics and functional mechanics of the T6 have been well studied[9], we know relatively little about how targeted cells respond, defend, and survive T6 attack. Similar to antibiotic resistance, one strategy is to neutralize the toxins. Bacteria wielding a T6 that

69 carries anti-microbial toxins do not intoxicate themselves or their sibling cells because a conjugate
70 immunity protein is encoded in the same gene cluster as each toxin[10–12]. However, cells lacking
71 immunity proteins are vulnerable to the toxins. In some cases, bacteria can acquire a library of
72 orphan immunity proteins via horizontal gene transfer and mobile genetic elements, enabling
73 them to survive toxins expressed by unrelated cells[13–16]. *Pseudomonas aeruginosa,* a model
74 organism for T6 research, is able to use cues from the environment to fight back against a T6-
75 wielding aggressor in two ways. In a "tit-for-tat" mechanism, cells that have been intoxicated by
76 T6 can then assemble their own apparatus and launch a counter-attack in the same direction from
77 which the first attack came[17,18]. *P. aeruginosa* is additionally able to induce T6 attack in response
78 to kin cell lysis, via a mechanism called "danger sensing"[19]. Physical processes can also offer
79 protection. Extracellular polysaccharide can protect cells from T6 attack, as does the
80 accumulation of cellular material from lysed cells and physical separation, which are both
81 consequences of T6 antagonism[20–23]. External signaling can play a role in this protection, with
82 recent reports that the presence of glucose enhances survival of *E. coli* cells to T6 attack,
83 mediated through cyclic AMP and its cognate target, the CRP regulator[24]. Other regulators that
84 coordinate stress response systems, such as Rcs and BaeSR may also play an important role,
85 as deletions of these genes reduces survival from attack[25,26]. Transposon sequencing (Tn-seq)[27]
86 offers one approach to identify genes that affect T6 resistance, uncovering mutations that either
87 increase or decrease survival[28]. However, this technique has a limited range of mutations it can
88 uncover, identifying only single null mutations contributing to a phenotype, but not deleterious
89 mutations in essential genes, functional point mutations, or epistatic relations between multiple
90 genes. Mutagenic screens also do not take pleiotropic side-effects of mutations into account. For
91 example, mutations that increase T6 survival but come at a steep cost to cellular growth rates
92 would be detected in such a screen, but might not be expected to arise under conditions where
93 reproductive fitness is important.

94 Experimental evolution[29] circumvents many of these issues, allowing interrogation of the
95 whole genome in a high-throughput, unbiased manner. By including periods of growth between
96 rounds of T6 attack, this approach allows selection to include key pleiotropic fitness effects. Clonal
97 interference among beneficial mutations means that only a small fraction of possible beneficial
98 mutations will arise to high frequency in any given experiment[30], typically favoring those that are
99 most adaptive. Rather than reporting all possible routes to surviving T6 attack, experimental
100 evolution thus provides insight into genetic mechanisms that provide the largest fitness advantage
101 over hundreds of generations of growth and periodic T6 assault.

102 In this paper, we explore how *E. coli* evolves resistance to T6 attack by *Vibrio cholerae*.
103 After ~500 generations of growth, punctuated by 30 rounds of attack by the T6, we identified two
104 main mutational pathways, each of which convergently evolved in multiple populations, that
105 enabled dramatically improved survival by *E. coli* during T6 attack. Similar to other types of
106 antibiotic resistance[31], we find that there was a strong trade-off between increased T6 survival
107 and reduced fitness during growth, which may help explain the continued efficacy of T6 antibiotics
108 in natural populations despite billions of generations of T6 exposure.

109

110 **Results**

111 *Experimental evolution of T6 resistance*

112 We report the development of an experimental evolution platform with two model
113 organisms, to identify mechanisms by which bacteria can become resistant to T6 attack (Fig. 1A).
114 We experimentally evolved eight replicate populations of *E. coli* MG1655, exposing them to daily
115 attack by a *V. cholerae* C6706 strain variant that constitutively expresses the building blocks of
116 the apparatus and its four T6 effectors, two that act in the periplasm to degrade the peptidoglycan
117 cell wall (VgrG3 and TseH) and two that disrupt membranes (TseL and VasX) (see Methods and
118 Materials)[12,32–34]. The two species were co-cultured on agar plates in 1:10 ratio (target to killer) to
119 ensure direct contact between cells, which is necessary for T6 attack. 99.99% of our *E. coli*

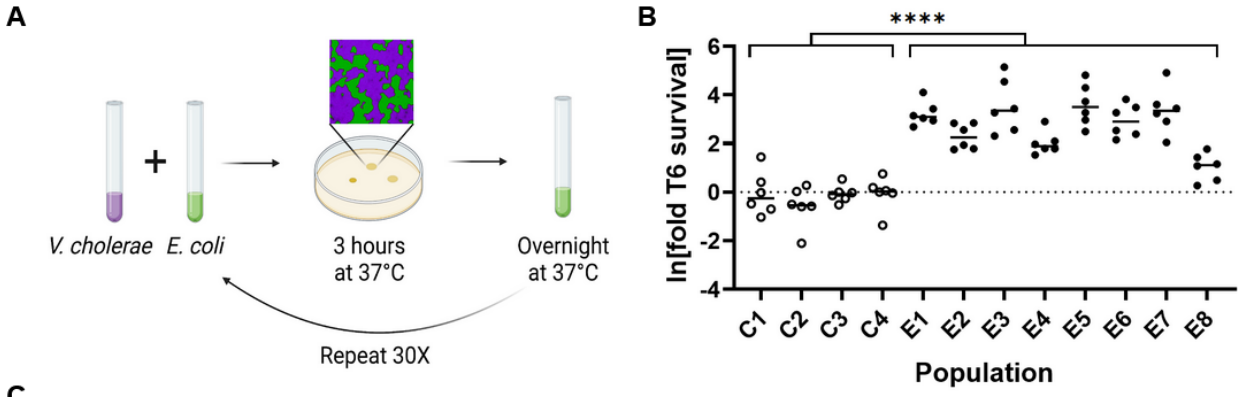

C

Gene	E1	E2	E3	E4	E5	E6	E7	E8
apaH **(280 AA; 840 nt)**	**Δ1 nt (121)**	**Δ13 nt (602-614)**		**Δ1 nt (359)**		**D37N**	**Δ4 nt (125-128)**	**W249X**
yjeP **(1107 AA; 3321 nt)**			**I724T**		**I724T**			
yejM **(586 AA; 1758 nt)**			**$(8bp)_{2\text{->}3}$***		**I427N**	**Q201L**		

Figure 1. Experimental evolution of resistance to *V. cholerae*'s Type VI Secretion System. (A) Experimental design. We experimentally evolved eight replicate populations of *E. coli*. Each round of selection included ~16 generations of growth in liquid media, followed by co-culture with T6-expressing *V. cholerae* on solid media, where initially the vast majority of *E. coli* were killed. *V. cholerae* were removed via antibiotics, and the surviving *E. coli* resumed growth in liquid media. (B) Over 30 rounds of selection, *E. coli* in the T6 treatment (solid circles) evolved a 27-fold increase in T6 survival, while controls competed against a T6(-) *V. cholerae* (open circles) did not evolve a significant increase in T6 resistance. **** denotes a difference in survival with $p \leq 0.0001$, determined via ANOVA and a pre-planned contrast. (C) Convergent evolution of genes affording T6 survival. Three genes were mutated in all eight independently evolving populations: *apaH* arose in six, while mutations in *yejM* and *yjeP* arose in the other two populations. For deletions (Δ), numbers in parentheses refer to the nt position of the deletion. $(8nt)_{2\text{->}3}$* refers to an 8 nt repeat that expanded from 2 repeats to 3 repeats long, resulting in a frameshift mutation. W249X refers to a premature stop codon at position 249, resulting in a protein product truncated near the C terminus. (AA = amino acids; nt = nucleotides).

---

ancestor were killed by *V. cholerae* during the solid-media killing phase of the experiment, imposing strong selection for T6 survival. Between rounds of competition, *E. coli* populations were grown for ~16 generations in LB medium overnight. We also evolved four control populations, competing the same ancestral *E. coli* against a T6-deficient *V. cholerae ΔvasK* strain. We reasoned that mutations arising in these four control populations would account for adaptation in our environment, including growth, dilution, and co-culture with *V. cholerae* on solid media, but not from injury from T6. After 30 rounds of selection, evolved strains were an average of ~27-fold

145 more resistant to *V. cholerae*'s T6 attack, and the control populations had on average 3.9% higher
146 survival, a negligible difference ($F_{11,71}$ = 15.8, $p \leq 0.0001$, ANOVA with replicate nested in
147 treatment. Fold survival was log-transformed prior to analysis to homogenize variances, and
148 treatment effect was assessed with pre-planned contrast, $F_{1,60}$ = 234, $p \leq 0.0001$; Fig. 1B).
149
150 *Identifying and characterizing key mutations*
151 We identified mutations arising in our experiment by sequencing a single genotype from
152 each population after 30 rounds of selection. With an average of 2.75 (standard deviation 1.09)
153 mutations per genome in the experimental populations, we chose to focus on mutations that
154 occurred in more than one replicate population, as convergent evolution strongly suggests these
155 mutations are adaptive (Fig. 1C, Fig. S1). Six of the eight isolates had mutations in *apaH*. Four of
156 which are frameshift mutations, suggesting they resulted in loss-of-function (Fig. 1C). This gene
157 is responsible for the "de-capping" of mRNAs in a bacterial cell[35]. Little is known about the global
158 regulatory effect of loss of *apaH*, but it is hypothesized that a null mutation leads to RNA
159 stabilization. Notably, the isolate from population E8 only gained a ~3-fold increase in survival
160 relative to its ancestor; which was significantly lower than five of the seven other replicate
161 experimental populations (Fold survival was log-transformed prior to analysis to homogenize
162 variances, pairwise differences between each replicate population assessed via ANOVA and
163 Tukey's HSD with overall significance at $\alpha = 0.05$; Fig. 1B). The mutation in *apaH* found in this
164 isolate creates a premature stop codon near the end of the gene (amino acid 249 out of 280) that
165 likely retains partial function of *apaH*, resulting in a more modest survival advantage.
166 Two of the eight isolates did not have a mutation in *apaH*. Instead, these two populations
167 each had missense or frameshift mutations in both *yjeP* (also known as *mscM*) and *yejM*,
168 suggesting an interaction between these two genes (Fig. 1C). *yjeP* encodes a mechanosensitive
169 channel that protects cells from osmotic shock[36]. The gene *yejM* (also known as *pbgA* and *lapC*)
170 encodes a metalloprotein that regulates bacterial lipopolysaccharides biosynthesis[37,38]. Deletion

171 of *yejM* is lethal in *E. coli*, while C-terminal truncation mutations result in partial function of the
172 gene[39]. Both mutations we found in *yejM* occur near the C-terminus.

173 To test the function of mutations found in *apaH*, *yjeP,* and *yejM* independent of the role of
174 other mutations that arose in experimental lineages (Fig. S1), we re-engineered mutations in
175 these genes in the ancestral strain. A clean deletion of *apaH* increases T6 protection by 3-fold,
176 whereas *E. coli* carrying a single copy of *apaH* expressed from a heterologous constitutive
177 promoter at the Tn7 site is 0.4-fold more susceptible than the ancestor (Fold survival was log-
178 transformed prior to analysis to homogenize variances, comparison of means was accessed with
179 one-sample t-test ($\mu = 0$) and Bonferroni correction with overall significance at $\alpha = 0.05$, $p \leq 0.0001$
180 and $p \leq 0.001$; Fig. 2A; see Methods and Materials).

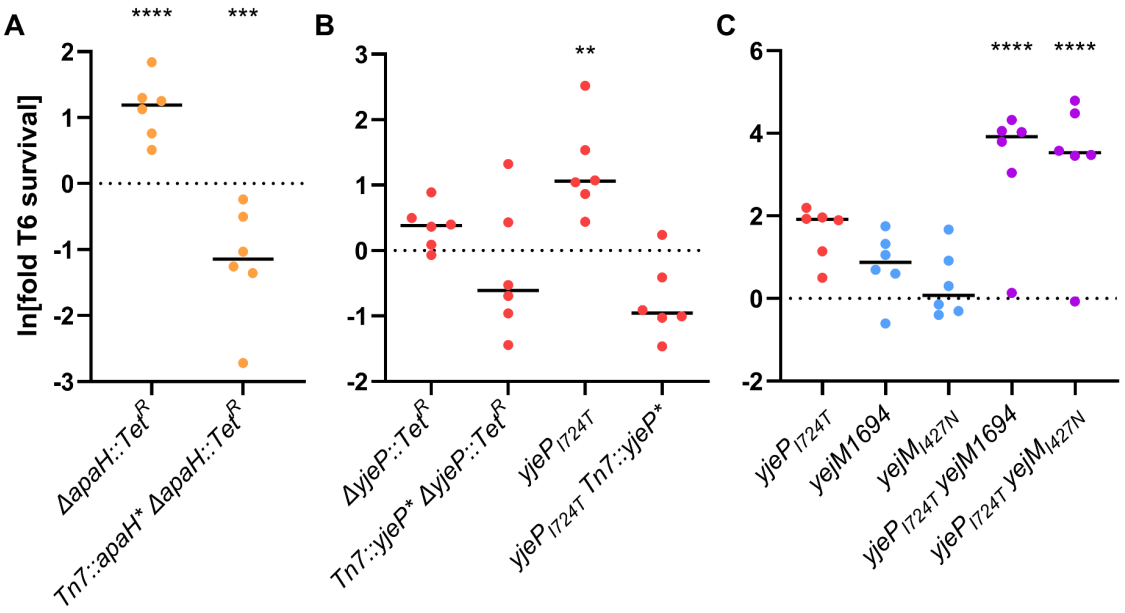

181

182 **Figure 2. While all mutations of interest increase T6 resistance in various degrees, the *yjeP/yejM***
183 **double mutants survive significantly better.** (A) *E. coli* with deletion of *apaH* or (B) *yjeP*$_{I724T}$ mutation
184 had a slight increase in T6 resistance that was not observed in the other variants. (C) The combination of
185 *yjeP*$_{I724T}$ and mutations in the C-terminus of YejM significantly improved the *E. coli* survival by more than
186 42-fold. Linked markers used to construct the mutants are not indicated in the figure. ****, ***, and ** denote,
187 differences in survival with $p \leq 0.0001$, $p \leq 0.001$, and $p \leq 0.01$ respectively, determined via ANOVA and
188 Dunnett's Multiple Comparison.
189
190 ----------

191
192 *yjeP$_{I724T}$ is a gain-of-function mutation that confers T6 resistance*

193 *yjeP* is one of four paralogs predicted to encode the MscS mechanosensory channel[36]. An
194 identical missense mutation in *yjeP* (*yjeP$_{I724T}$*) occurred independently in two lineages (Fig. 1C),
195 suggesting that this amino acid substitution enhances T6 survival and represents a gain-of-
196 function mutation. In the ancestor genetic background, we introduced a *yjeP* disruption,
197 constitutively expressed *yjeP,* and reconstructed the *yjeP$_{I724T}$* mutation. Interestingly, neither the
198 absence of *yjeP* nor its constitutive expression affected T6 survival. However, *E. coli* carrying the
199 *yjeP$_{I724T}$* mutation experienced a ~4-fold survival benefit (Fold survival was log-transformed prior
200 to analysis to homogenize variances, pairwise differences between each replicate population
201 assessed via ANOVA and Dunnett's test with overall significance at $\alpha = 0.05$, $p \leq 0.01$; Fig. 2B).

202 Because YjeP is predicted to be a mechanosensitive channel[36], we determined how the
203 *yjeP$_{I724T}$* mutant responded to pH and osmotic shock, classic stressors for probing
204 mechanosensor function. A *yjeP* null mutant behaved like WT. Interestingly, while the *yjeP$_{I724T}$*
205 mutant *w*as unaffected by changes in osmolarity, it did exhibit 1.1- to 1.4-fold decreases in
206 maximum growth rate in the exponential phase, which was more pronounced with potassium,
207 suggesting that the YjeP may be an ion channel (OD_{600} was log-transformed prior to analysis, and
208 the pH effect was assessed with linear regression comparison of the slopes in the exponential
209 phase with significance at $\alpha = 0.05$; Fig. 3). To determine whether YjeP is the only MscS
210 mechanosensitive channel protein that can affect T6 resistance, we also tested one of three YjeP
211 homologs, YbdG[36], because a prior study showed a *ybdG$_{I176T}$* gain-of-function mutation also
212 confers sensitivity to osmotic shock[40]. Unlike *yjeP$_{I724T}$*, the *ybdG$_{I167T}$* did not confer T6 resistance,
213 nor did a *ybdG* null (Fig. 3; Fig. S2). Thus, we conclude that *yjeP$_{I724T}$* is a gain-of-function, or co-
214 dominant, mutation in an ion channel that confers T6 resistance.

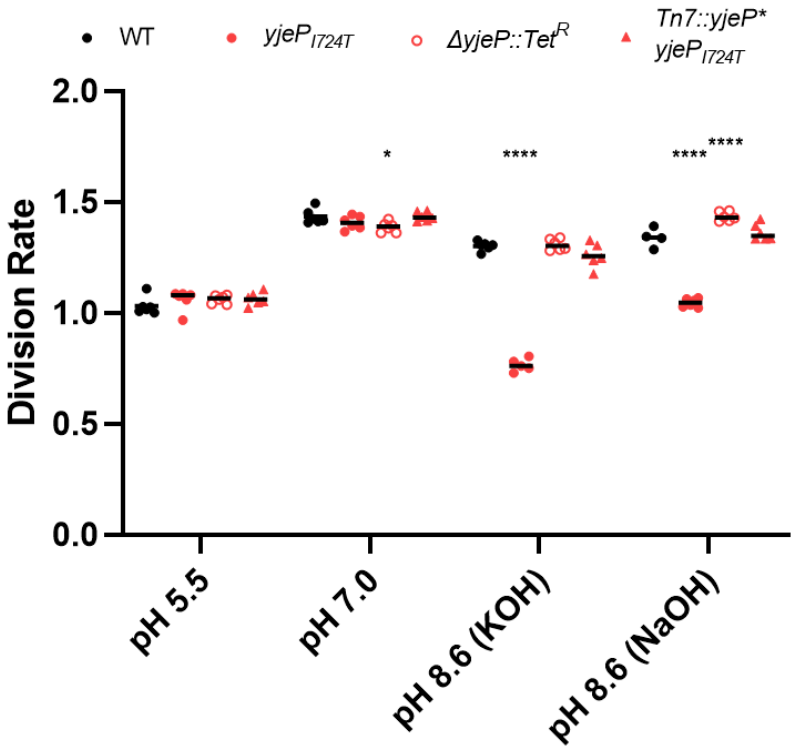

Figure 3. *E. coli yjeP$_{I724T}$* has reduced fitness under basic conditions. *E. coli* and its *yjeP* derivatives grow similarly under acidic and neutral pH. In basic media, however, the *yjeP$_{I724T}$* mutant has a significant decrease in division rate. Linked markers used to construct the mutants do not affect growth in the tested conditions (Fig. S3). ****, **, and * denote, differences in survival with $p \leq 0.0001$, $p \leq 0.01$, and $p \leq 0.05$ respectively, determined via Two-way ANOVA and Dunnett's Multiple Comparison.

E. coli yjeP/yejM double mutants are much more resistant to novel T6 toxins

The fact that *yejM* and *yjeP* accrued mutations in parallel in two independent populations suggests there may be an epistatic relationship between these two mutations. To test this hypothesis, we introduced both *yejM* mutations into the ancestral *E. coli* without and with the *yjeP$_{I724T}$* mutation. While the *yjeP$_{I724T}$* mutation confers a modest benefit (4-fold increased survival; fold survival was log-transformed prior to analysis to homogenize variances, pairwise differences between each replicate population assessed via ANOVA and Dunnett's test with overall significance at $\alpha = 0.05$, $p \leq 0.01$; Fig. 2B), the presence of either *yejM* mutation by itself has no

234 effect on resistance (Fig. 2C). However, the *yjeP*$_{I724T}$ mutation combined with either *yejM* mutation
235 enables a ~40-50-fold increase in survival compared to the ancestor (fold survival was log-
236 transformed prior to analysis to homogenize variances, pairwise differences between each
237 replicate population assessed via ANOVA and Dunnett's multiple comparison with overall
238 significance at $\alpha = 0.05$, $p \leq 0.0001$; Fig. 2C). In other words, mutation in *yejM* increases resistance
239 only in strains that also have the *yjeP* point mutation.

240 We next examined whether the mutations that arose in our experiment provide general
241 resistance to T6 attack, or are specific to the toxins employed by the *V. cholerae* C6706 strain,
242 used in this evolution screen, which codes three auxiliary T6 effectors in addition to the large
243 cluster. We therefore competed each mutant *E. coli* strain against an environmental isolate of *V.*
244 *cholerae* killer, BGT41 (also known as VC22), which encodes a constitutive T6 with effectors
245 predicted to have enzymatic activities distinct from those produced by C6706 and encountered
246 by *E. coli* during experimental evolution[41,42]. This environmental isolate is a superior killer of *E.*
247 *coli*, relative to C6706[42], necessitating that we perform our killing assays at a 1:4 killer:target ratio,
248 rather than the 10:1 ratio used with C6706. Evolved strains with *yjeP*$_{I724T}$ and *yjeP*/*yejM* double
249 mutations survived 4,000-fold better than the *E. coli* ancestor, but *apaH* did not measurably
250 increase survival (Fold survival was log-transformed prior to analysis to homogenize variances,
251 pairwise differences between each replicate population assessed via ANOVA and Dunnett's
252 multiple comparison with overall significance at $\alpha = 0.05$, $p \leq 0.0001$; Fig. 4). In addition, unlike with
253 C6706 killer (Fig. 2C), the *yejM* mutations did not further increase the survival of the *yjeP*$_{I724T}$
254 mutant (Fig. 4). This suggests that I724T in *yjeP* may provide broad spectrum resistance to T6
255 while protection conferred by mutations in the YejM C-terminus and in *apaH* may depend on the
256 specific effector employed.
257
258

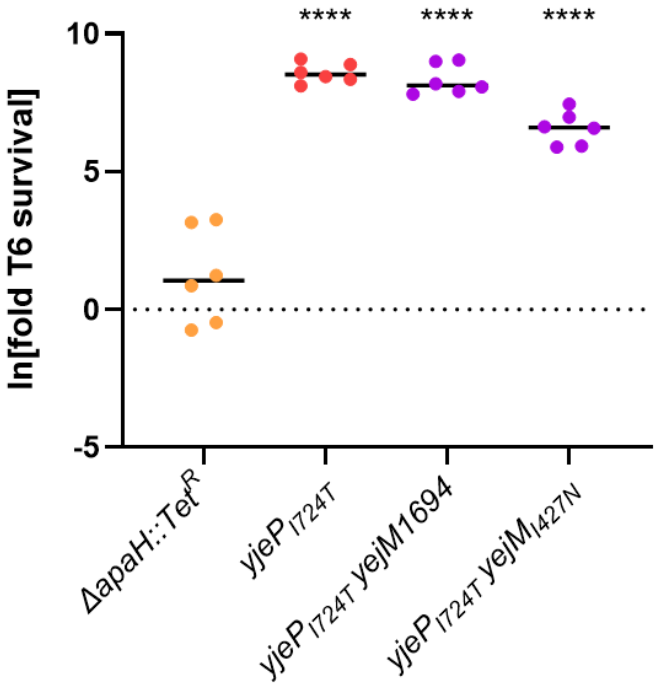

Figure 4. The *yjeP* and the *yjeP/yejM* mutants provide general resistance to T6 attack. When competed against *V. cholerae* with a set of toxins not encountered during experimental evolution, *E. coli* mutants with *yjeP*$_{I724T}$ had an increase of >250-fold in T6 resistance whereas deletion of *apaH* did not provide protection against novel T6 effectors. Linked markers used to construct the mutants are not indicated in the figure. **** denotes a difference in survival with $p \leq 0.0001$, determined via ANOVA and Dunnett's Multiple Comparison.

Experimental evolution reveals trade-offs between T6 resistance and growth rate

So far we have shown that *E. coli* readily evolves resistance to T6 attack, one of the most common mechanisms of antimicrobial warfare. Why, after billions of years of evolution, are bacteria still so poorly defended against T6? Evolutionary theory predicts that trade-offs between antibiotic resistance and other fitness-dependent traits can maintain susceptibility[43]. To test this hypothesis, we examined the effect of each mutation on cellular growth rate by competing them against the ancestral genotype of *E. coli*, under the conditions that mirrored our selection experiment. Mutations in *apaH*, *yejM*, and *yjeP* decreased fitness during growth (Fig. 5). In fact, there was an overall negative correlation between T6 survival and growth rate for the strains generated in this study ($log_{10}(survival) = -2.988\ log_{10}(growth) - 0.2698$, R^2=0.65, p=3.01*10^{-5}; this

280 regression excludes the *crp* and *rlmE* mutants, which never arose during experimental evolution;
281 Fig. 5A).

282 Our evolution experiment consisted of ~16 generations of exponential growth in LB media,
283 followed by T6 killing. We thus calculated a fitness isocline across the phase space of this trade-
284 off (black dashed line in Fig. 5A), along which a mutant would have equal fitness to the ancestor
285 across one round of growth and killing, with the equation $y = 1/x$ (in $\log_{10}$ space). For example,
286 along this line, a 100-fold increase in T6 survival is exactly canceled out by a 100-fold decrease
287 in overnight growth. Mutations that lie above this line should be more fit than our ancestral strain,
288 while mutations below the line should be maladaptive. Perhaps unsurprisingly, given the strong
289 selection on both growth and T6 survival, all mutations we identified are adaptive.

290 We also measured growth and survival rates for two disruptive mutations that did not arise
291 in our experimentally evolved populations - *crp* and *rlmE*. We have previously shown that deletion
292 of *crp*, a global transcriptional repressor, results in increased survival to the T6 in *E. coli*, but also
293 greatly reduces growth rate[24,44,45]. While this mutation does fall above the fitness isocline, it did
294 not appear in our evolution experiment (Fig. 5). Because all of our mutations of interest result in
295 decreased growth rate, we also sought to test whether decreased growth rate was sufficient to
296 increase T6 resistance. For example, slower growth could prevent microcolonies of the two strains
297 from physical contact on the plate during the course of the co-culture competition. We constructed
298 an *E. coli* strain with a *rlmE* deletion, which grows ~0.14% as much as the ancestor during one
299 round of growth (t-test $p=8.75*10^{-5}$). This strain results in much smaller colonies when growing on
300 plates, but has only a 10-fold increase in survival when challenged with T6 attack (Fig. S4). The
301 *rlmE* mutant is below the fitness isocline in Fig. 4A, as the modest increase in survival is not
302 commensurate with the huge growth defect of this mutant if slower growth always led to higher
303 T6 resistance. This shows that slower growth is a side-effect of mutations that increase T6
304 resistance, not a cause of increased resistance.

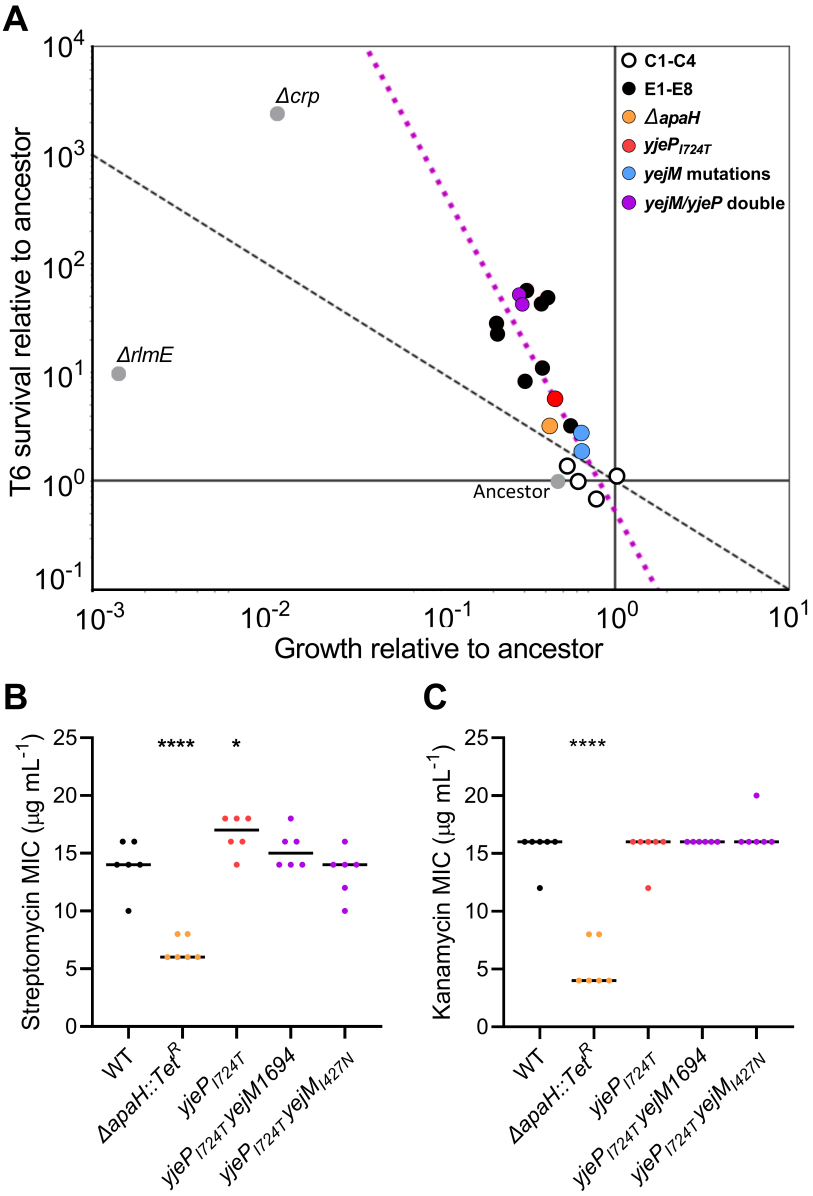

Figure 5. Trade-offs between T6 resistance and fitness during growth. (A) Mutations conferring a larger T6 survival advantage also resulted in a greater reduction to reproductive fitness. Plotted are the change in frequency of each mutant across one 16 generation growth assay, and one T6 attack, following the protocols from our evolution experiment. The dashed line represents a fitness isocline, $y = 1/x$, where fitness across one round of selection is equal to that of the ancestor. In other words, the isocline represents where increased fitness during T6 survival is exactly outweighed by decreased fitness in the growth phase. The pink dashed line represents correlation between survival benefit and growth cost; $log_{10}(survival) = -2.988\ log_{10}(growth) - 0.2698$, $r^2=0.65$, $p=3.01*10^{-5}$. Green: reconstructed mutations; Red: Evolved isolates; Blue: evolution controls. **(B,C)** Disruption of *apaH* results in decreased MIC for streptomycin (B) and kanamycin (C). The point mutation *yjeP*$_{I724T}$ does not affect susceptibility to these antibiotics. Linked markers used to construct the mutants are not indicated in the figure. **** and * denote differences in survival with $p \leq 0.0001$ and $p \leq 0.05$, determined via ANOVA and Dunnett's Multiple Comparison.

318
319 Another trade-off we tested is susceptibility to aminoglycoside antibiotics. The *apaH*
320 disruption strain has a significantly lower minimum inhibitory concentration (MIC) than the
321 ancestor when grown in streptomycin and kanamycin (pairwise differences between each
322 replicate population assessed via ANOVA and Dunnett's test with overall significance at $\alpha = 0.05$,
323 $p \leq 0.0001$ and $p \leq 0.05$; Fig. 5B-C), meaning that they are more susceptible to these antibiotics.
324 This is consistent with previous work on *apaH*[46]. However, strains containing the *yjeP* point
325 mutation did not show increased susceptibility.
326
327 **Discussion**
328 In this paper, we use experimental evolution to examine how bacteria adapt to frequent
329 T6 exposure. We subjected populations of *E. coli* to alternating selection for rapid growth followed
330 by attack by *V. cholerae*'s T6 (Fig. 1A). All replicate populations evolving increased T6 resistance
331 (seven of the eight populations) utilized one of two pathways: either a loss-of-function mutation in
332 *apaH*; or a gain-of-function mutation I724T in *yjeP* combined with a partial loss-of-function in *yejM*,
333 with both mutations necessary to provide a large survival advantage (Fig. 1B-C). For a $yjeP_{I724T}$
334 mutant, the protection appears to be broad-spectrum, increasing resistance to novel effector
335 proteins by more than 3,000-fold (Fig. 4). Interestingly, the *yjeP*/*yejM* double mutants are also
336 comparatively resistant to T6 when competing against *V. cholerae* BGT41 (Fig. 4), suggesting
337 $yjeP_{I724T}$ provides a broader protection while the additional yejM mutations are specific to C6706
338 T6 effectors (Fig. 2C). While the mechanism underpinning this strain-specific effect is beyond the
339 scope of this study, we hypothesize $yejM_{I427N}$ still encodes a partially functional YejM periplasmic
340 domain, whereas an insertion of 8 nt (*yejM*1694) results in a frameshift mutation, resulting in a
341 complete disruption of the C-terminus[47]. In *Salmonella enterica and E. coli,* truncation of the C-
342 terminus was shown to disrupt the function of YejM, negatively impacting lipopolysaccharide
343 biosynthesis. This leads to a defective outer membrane that leaks periplasmic proteins into the
344 extracellular space[48]. Periplasmic leakage may reduce the concentration of membrane-localized

345 T6 toxins injected into *E. coli* bearing the *yejM*1694 mutation, reducing their lethality. In contrast,
346 mutations in *apaH* were specific to the T6 effectors they were evolved against, showing no efficacy
347 against a different strain of *V. cholerae* with novel T6 effectors (Figs. 2A, 4).

348 Of the two primary mutational pathways we focused on in this study, it is interesting that
349 the less beneficial path to T6 resistance, loss of function in *apaH,* evolved more times than the
350 far more beneficial combination of $yjeP_{I724T}$ and a partial loss-of-function of *yejM* (Fig. 4). This is
351 likely because it is easier to gain beneficial mutations in the *apaH* pathway: any loss of function
352 mutation in the gene gives the phenotype, whereas the *yejM/yejP* pathway requires mutations in
353 two separate genes. The convergent evolution we observed in our experiment (identical *yjeP*
354 SNPs in both populations evolving resistance via this mechanism) further suggests that specific
355 mutations, not simple loss of function mutations, may be required in *yjeP.* Given the difference in
356 T6 resistance between evolved isolates with an *apaH* mutation (Fig. 1B,C) and the constructed
357 *apaH* mutant (Fig. 2A), we hypothesize that other mutations acquired by the evolved populations
358 may also contribute to T6 survival.

359 Over 500 generations of experimental evolution in 8 replicate populations, we found just
360 two pathways to increased T6 resistance. While prior work has shown that many genes that can
361 affect T6 survival[25,28,49–51] implying that adaptation might be idiosyncratic among independent
362 populations, our results suggest that adaptive routes to T6 resistance are remarkably constrained.
363 One possibility is that our populations are mutationally limited. This is unlikely, as we can expect
364 ~9.2×10^5 mutations to arise within each growth cycle (based on ~10^{10} cells being produced per
365 cycle, a per base mutation rate of ~(0.2×10^{-10})[52] and a genome size of 4.6 MB), or 2.8×10^7
366 mutations in each population over the course of the experiment. Instead, the high degree of
367 evolutionary convergence in our experiment suggests that there may simply be relatively few
368 routes to increased T6 survival in which the benefits of the mutation, integrated across the culture
369 cycle to include pleiotropic costs, are great enough to drive the clonal lineage to high frequency.

370 The evolution of resistance to diffusible antibiotics has been extensively studied[53]. While
371 the details depend on taxon and environment[54,55], antibiotic resistance often comes with trade-
372 offs to other fitness components[54–57]. This is especially true for mutations in essential genes that
373 are the target of antibiotics, such as genes encoding ribosomal proteins[58]. However,
374 compensatory evolution often reduces initially severe costs of resistance, either via the fixation of
375 epistatic mutations elsewhere in the genome, or by replacing initially costly resistance mutations
376 with lower-cost alternatives[58–61]. In contrast to diffusible antibiotics, the eco-evolutionary dynamics
377 of contact-mediated killing remains largely unexplored, and it is unclear if or when similar
378 compensatory adaptation would occur if we continued our experiment. The fact that we observe
379 a strong trade-off between T6 survival and growth rate is not entirely unexpected. The T6
380 secretion system is an ancient, widespread, and highly effective microbial weapon. Trade-off free
381 adaptations that increase survival to T6 attack would be expected to rapidly fix in many bacterial
382 populations. As a result, pleiotropic costs to T6 resistance could play an important role in
383 maintaining T6 efficacy over evolutionary time.

384 Single mutations that confer resistance to an individual antibiotic are common, as a
385 modification of one target site may be sufficient to escape drug toxicity[62]. Because the probability
386 a susceptible cell will simultaneously gain mutations allowing it to survive multiple antibiotics is
387 far lower than the probability of gaining resistance to any single antibiotic, physiological
388 mechanisms that afford broad-spectrum toxin resistance (e.g., efflux pumps) can often incur
389 fitness trade-offs[63]. Current efforts to combat antibiotic resistance appropriately focus on
390 identifying drug targets that incur large fitness costs; with modern drug combination, drug cycling,
391 and adaptive therapies seeking to exploit these fitness trade-offs to slow the rate of resistance
392 evolution[64–67]. We thus might expect that, as in our experiment here, T6 resistance often evolves
393 via mechanisms that modify cellular physiology or behavior (e.g., increased capsule thickness)
394 that improves survival, albeit with pleiotropic costs[21]. In contrast to diffusible antibiotics, it may be
395 more difficult for bacteria to evolve resistance to T6-delivered antibiotics. T6 attacks

396 synchronously deliver multiple effectors that target different components of the intoxicated cell,
397 and delivery is direct, which minimizes dilution and dispersal of the toxins in a heterogenous
398 extracellular environment.

399 It has only recently become apparent how important social interactions are to microbial
400 ecology and evolution[68,69]. Antagonistic interactions appear to be more common than cooperation
401 or commensalism[1], at least for species that are capable of being cultured. The Type VI secretion
402 system - a ballistic harpoon containing multiple types of toxins capable of quickly killing
403 susceptible cells, represents the cutting-edge of microbial weaponry. In this paper, we show that
404 *E. coli* can indeed evolve substantial genetic resistance to T6 assault, but doing so entails trade-
405 offs with reproductive fitness. We also found that one convergently-evolving solution appeared to
406 provide effector-specific protection, while the other appeared to be more general. So far, relatively
407 little effort has gone into understanding the mechanisms (both genetic and behavioral) through
408 which microbes can evolve to resist dying from T6- a crucial gap in our knowledge that limits our
409 ability to understand the ecology and evolution of this widespread microbial weapon. Further work
410 will be required to determine if trade-offs between T6 survival and reproduction are found in other
411 taxa, and whether such trade-offs can be mitigated over longer evolutionary timescales via
412 compensatory mutation.

413

414 **Materials and Methods**

415 *Bacterial strains and media*

416 Bacterial strains were grown aerobically at 37 °C overnight in lysogeny broth (LB) (1% w/v
417 tryptone (Teknova, CA, USA), 0.5% w/v yeast extract (Hardy Diagnostics, CA, USA), 1% w/v NaCl
418 (VWR Life Sciences, PA, USA) or liquid basal medium (100 mM Tricine (Thermo Scientific, MA,
419 USA), 10 mM K_2HPO_4 (Fisher Scientific, NH, USA), 0.5% w/v tryptone, 0.25% w/v yeast extract,
420 0.5% w/v glucose (VWR, PA, USA), and pH 5.5 with HCl (Fisher Scientific, NH, USA) or pH 8.6
421 with KOH (Fisher Scientific, NH, USA) or NaOH (Fisher Scientific, NH, USA)) with constant

422 shaking or on LB agar (1.5% w/v agar; Genesee Scientific and Hardy Diagnostics, CA, USA).
423 Ampicillin (GoldBio, MO, USA and VWR Life Sciences, PA, USA), spectinomycin (Sigma-Aldrich,
424 MO, USA and Enzo Life Sciences, NY, USA), streptomycin (VWR Life Sciences, PA, USA),
425 kanamycin (GoldBio, MO, USA and VWR Life Sciences, PA, USA), chloramphenicol (Sigma-
426 Aldrich, MO, USA and EMD Millipore, MA, USA), tetracycline (Sigma-Aldrich, MO, USA and
427 Fisher BioReagents, PA, USA), and arabinose (GoldBio, MO, USA) were supplemented where
428 appropriate. Specific concentrations will be described below.
429
430 *Mutant construction*
431 Mutations were introduced into *E. coli* K-12 strain MG1655 Δ*araBAD*::*cat* by P1vir transduction[70].
432 Point mutations in *ybdG*, *yejM*, and *yjeP* were transduced into the recipient strain using the
433 genetically linked markers *purE*79::Tn10, zei-722::Tn10, and Δ*yjeJ*::*ampR*, respectively.
434 Transductants were selected for using 10 μg mL^{-1} tetracycline or 25 μg mL^{-1} ampicillin and
435 screened for the presence of the point mutations by DNA sequencing (Azenta Life Sciences, MA,
436 USA). All null mutations were confirmed by PCR.
437 *yjeJ* and *rlmE* were deleted and replaced with the Amp^R or Tet^R cassette, respectively, by λ Red
438 recombination as previously described[71]. To generate Δ*yjeJ*::*ampR,* the Amp^R cassette from
439 pUC19 was amplified by PCR using the primers KOyjeJBla.Fwd and KOyjeJBla.Rev, which
440 contain homology to the 5' and 3' ends of *yjeJ*, respectively. To generate Δ*rlmE*::*tetA*, the *tetA*
441 gene and promoter were amplified from Tn10 using the primers rrmJTET.Fwd and rrmJTET.Rev.
442 Δ*yjeJ*::*ampR* or Δ*rlmE*::*tetA* DNA were transformed into DY378, a strain of *E. coli* K-12 that
443 expresses the λ Red recombination system from a temperature sensitive promoter. Prior to
444 transformation, the λ Red system was induced by incubating midlog phase DY378 cells at 42°C
445 for 15 minutes in a shaking water bath. Recombinants were selected for on LB containing 25 μg
446 mL^{-1} ampicillin (for Δ*yjeJ*::*ampR*) or 10 μg mL^{-1} tetracycline (for Δ*rlmE*::*tetA*).

447 To generate the Δ*apaH*::*tetA*, Δ*ybdG*::*tetA*, and Δ*yjeP*::*tetA* null alleles, Δ*apaH*::*ampR*,
448 Δ*ybdG*::*kanR*, and Δ*yjeP*::*kanR* from the Keio library[72] were moved into DY378 by P1vir
449 transduction[70]. The Kan^R cassette in each Keio allele was replaced with *tetA* from Tn10 by λ Red
450 recombination[71]. The *tetA* DNA was amplified by PCR using the primers pKD13TetA.Fwd and
451 pKD13TetA.Rev, which contain homology to the 5' and 3' ends of the Kan^R cassette, respectively.
452 Recombinants were selected for on LB containing 10 μg mL^{-1} tetracycline and screened for
453 sensitivity to 25 μg mL^{-1} kanamycin.
454 $ybdG_{I167T}$ was constructed using CRISPR-Cas9 gene editing as previously described[73]. The *ybdG*
455 guide RNA plasmid pCRISPR-ybdG493 was constructed by ligating ybdG493.CRISPR duplexed
456 DNA (Integrated DNA Technologies, IA, USA) into BsaI-digested pCRISPR. 100 ng of pCRISPR-
457 ybdG493 and 10 uM of the editing oligonucleotide ybdGI167T.MAGE (Integrated DNA
458 Technologies, IA, USA) were transformed into MG3686, a derivative of DY378 that constitutively
459 expresses Cas9 from a plasmid. Transformants were selected for on LB containing 25 μg mL^{-1}
460 chloramphenicol and 50 μg mL^{-1} kanamycin. Recombinants containing the $ybdG_{I167T}$ mutation
461 were identified by DNA sequencing (Azenta Life Sciences, MA, USA). Two phosphorothioate
462 bonds were added at the 5' and 3' ends of the ybdGI167T.MAGE oligonucleotide to increase
463 stability.
464 Genes were inserted at the Tn7 attachment site following a similar protocol described
465 previously[74,75]. Wildtype *apaH* or *yjeP* expressed from the constitutive promoter J23119
466 (http://parts.igem.org/Part:BBa_J23119) were cloned into XhoI and HindIII (New England Biolabs,
467 MA, USA) digested pZS21, resulting in the plasmids pZS21-*apaH* and pZS21-*yjeP*. The J23119
468 promoter, gene, and *rrnB*1 terminator from pZS21-*apaH* or pZS21-*yjeP* were amplified by PCR
469 using the primers pGRG25GA.Fwd and pGRG25GA.Rev. The Ω streptomycin/spectinomycin
470 resistance cassette from pHP45Ω was amplified using the primers pGRG25SpcGA.Fwd and
471 pGRG25SpcGA.Rev. *apaH* or *yjeP* DNA along with DNA corresponding to the Ω
472 streptomycin/spectinomycin resistance cassette were inserted into PacI and AvrII digested

473 pGRG25-ModularBamA-Kan by Gibson Assembly (New England Biolabs, MA, USA). The
474 resulting plasmids were transformed into MG1655 and transformants were selected for on LB
475 containing 25 μg mL^{-1} spectinomycin and 0.2% (w/v) arabinose. Transformants were screened
476 for integration of *apaH* or *yjeP* and the Ω streptomycin/spectinomycin resistance cassette at the
477 Tn7 site by PCR.
478 *V. cholerae* was genetically engineered with established allelic exchange methods using vector
479 pKAS32[76]. Expression of chromosomal *qstR* from a heterologous Ptac promoter results in
480 constitutive T6 activity because C6706 lacks a functional *lacI* gene[77]. An in-frame deletion of *vasK*
481 tprevents T6 assembly, as described previously[13]. All Insertions, deletions, and mutations were
482 confirmed by PCR and DNA sequencing (Eton Bioscience Inc, NC, USA).
483
484 *Experimental evolution*
485 Twelve replicate populations of *E. coli* with chloramphenicol (10 μg mL^{-1}) were initiated from an
486 overnight culture of MG1655 with chromosomal Cm^R cassette and a plasmid encoding Kan^R
487 cassette. Each round, cultures were washed twice with LB to remove antibiotics, then mixed with
488 an overnight culture of either *V. cholerae* C6706 *qstR** (for the 8 experimental populations) or
489 C6706 *qstR** Δ*vasK* (for the 4 control populations) in a 10:1 killer to target ratio. 50 μL of each
490 mixture was spotted onto an LB agar plate, dried, and incubated at 37°C for 3 hours. Competition
491 mixtures were then resuspended in 5 mL of ddH_2O containing kanamycin (50 μg mL^{-1}) and
492 chloramphenicol (10 μg mL^{-1}), and put at 4°C for 30 minutes, conditions which allow for survival
493 of *E. coli* but not *V. cholerae*. Surviving cells were then diluted 10-fold into LB containing
494 kanamycin (50 μg mL^{-1}) and chloramphenicol (10 μg mL^{-1}) for overnight growth at 37°C. This
495 procedure was repeated daily for 30 rounds. A sample of each whole population was frozen at -
496 80°C every five rounds. At the end of 30 rounds, a clonal isolate from each population was taken
497 for subsequent phenotypic and genomic testing.
498

499 *Stress assay*

500 The optical density (OD_{600}) of overnight cultures of *E. coli* strains growing in the basal medium
501 (pH 7) was measured by a ThermoFisher Scientific Genesys 30 spectrophotometer (MA, USA)
502 and normalized to 1. Then cells were diluted 1:50 into the basal medium (pH 5.5, pH 7, and pH
503 8.6 with KOH or NaOH) in a 96-microtiter plate, which was incubated aerobically at 37 °C with
504 shaking in a BioTek Synergy H1 microplate reader (VT, USA). The OD_{600} of each well was read
505 every 30 mins for 16 h. A curve of best fit was assigned to each well using the 4P Growth model
506 in JMP (JMP®, Version 16.1.0. SAS Institute Inc., Cary, NC, 1989–2021), and the value of the
507 "Division" parameter was compared across treatments and replicates.

508

509 *Antibiotic minimum inhibitory concentration (MIC) determination*

510 Antibiotics were added to wells of a 96-microtiter plate, starting at 1280 µg mL^{-1} for streptomycin
511 and 640 µg mL^{-1} for kanamycin, and serially diluted 2-fold across the plate. Overnight cultures of
512 bacteria were diluted and added to the wells for a final OD_{600} of 0.001. Once a target range was
513 determined to contain the MIC for each antibiotic, a linear range of antibiotic concentrations were
514 prepared and tested in 96-microtiter plate (4 through 36 µg mL^{-1} for kanamycin and 2 through 18
515 µg mL^{-1} for streptomycin), and bacteria were added at a an OD_{600} of 0.001. Plates were incubated
516 stationary at 37°C for 24 hours. A well was determined to have growth if the OD_{600} was above
517 0.2, as measured by a BioTek Synergy H1 microplate reader (VT, USA), and the MIC was
518 determined to be the lowest concentration at which no growth occurred.

519

520 *T6-mediated competition assay*

521 The OD_{600} of overnight cultures of *V. cholerae* killer and Cm^R *E. coli* target were normalized to 1.
522 Killer and target are then mixed in either 10:1 or 1:4 ratio, inoculated onto a pre-dried LB agar,
523 and allowed to dry. After 3 hours of static incubation at 37°C, cells were resuspended in 5 ml of
524 LB, following with serial dilutions. Finally, the resuspension was inoculated on a LB agar

525 containing chloramphenicol (10 μg mL^{-1}) to select for the surviving *E. coli*, which was incubated
526 overnight at 37 °C and the *E. coli* colonies were counted. Data is presented as the fold increase
527 of the survival rate for a given genotype as compared to the ancestor (measured in the same
528 experiment), as given by:

529 $$Fold\ increase\ = \frac{Survival\ rate\ of\ genotype}{Survival\ rate\ of\ ancestor},$$

530 where the survival rate for each strain is calculated by dividing recovered *E. coli* colonies from
531 competition with the T6+ *V. cholerae* strain by the number of colonies recovered from competition
532 with the T6- strain.
533
534 *Genomic DNA preparation, whole genome sequencing, and genomic analysis*
535 *E. coli* genomic DNA from each population was isolated using Promega Wizard Genomic DNA
536 Purification Kit (Madison, WI). The DNA quality was analzyed using gel electrophoresis to confirm
537 no degradation and NanoDrop to confirm the purity of the samples (260/280 = 1.8-2.0). Whole
538 genome sequencing was conducted using Illumina sequencing on a NextSeq 2000 platform at
539 Microbial Genome Sequencing Center (PA, USA). Once we received the DNA sequencing results,
540 quality check, filter, base correction, adapter trimming, and merging were conducted using fastp
541 v0.20.0[78]. Reads were then mapped and compared to the *E. coli* MG1655 reference genome
542 (accession U00096) from NCBI Genome database using Breseq v0.35.1 with bowtie2-stage2[79–
543 81]. Other parameters remain default.
544
545 **Acknowledgments and funding sources**
546 Figure 1A was made using Biorender.com. K.M. is supported by NIH T32 grant T32GM142616.
547 SLN is supported by NSF grant BMAT 2003721.
548
549 We declare no conflict of interest.

550

551 **Data availability:**

552 In addition to the data from this study included in the article and/or supporting information,

553 genomes sequence will be posted to the NCBI short read archive upon acceptance of the

554 manuscript.

555 **References**

556 1. Palmer, J. D. & Foster, K. R. Bacterial species rarely work together. *Science* **376**, 581–582
557 (2022).
558 2. Aminov, R. I. The role of antibiotics and antibiotic resistance in nature. *Environ. Microbiol.*
559 **11**, 2970–2988 (2009).
560 3. Hall, S. *et al.* Cellular Effects of Pyocyanin, a Secreted Virulence Factor of Pseudomonas
561 aeruginosa. *Toxins* **8**, 236 (2016).
562 4. Michalska, M. & Wolf, P. Pseudomonas Exotoxin A: optimized by evolution for effective
563 killing. *Front. Microbiol.* **6**, (2015).
564 5. Rabin, S. D. P. & Hauser, A. R. Pseudomonas aeruginosa ExoU, a Toxin Transported by
565 the Type III Secretion System, Kills Saccharomyces cerevisiae. *Infect. Immun.* **71**, 4144–
566 4150 (2003).
567 6. Pukatzki, S. *et al.* Identification of a conserved bacterial protein secretion system in Vibrio
568 cholerae using the Dictyostelium host model system. *Proc. Natl. Acad. Sci. U. S. A.* **103**,
569 1528–1533 (2006).
570 7. Boyer, F., Fichant, G., Berthod, J., Vandenbrouck, Y. & Attree, I. Dissecting the bacterial
571 type VI secretion system by a genome wide in silico analysis: what can be learned from
572 available microbial genomic resources? *BMC Genomics* **10**, 104 (2009).
573 8. MacIntyre, D. L., Miyata, S. T., Kitaoka, M. & Pukatzki, S. The Vibrio cholerae type VI
574 secretion system displays antimicrobial properties. *Proc. Natl. Acad. Sci.* **107**, 19520–19524
575 (2010).
576 9. Crisan, C. V. & Hammer, B. K. The Vibrio cholerae type VI secretion system: toxins,
577 regulators and consequences. *Environ. Microbiol.* **22**, 4112–4122 (2020).
578 10. Yang, X., Long, M. & Shen, X. Effector–Immunity Pairs Provide the T6SS Nanomachine its
579 Offensive and Defensive Capabilities. *Molecules* **23**, 1009 (2018).
580 11. Miyata, S. T., Unterweger, D., Rudko, S. P. & Pukatzki, S. Dual expression profile of type VI

581 secretion system immunity genes protects pandemic Vibrio cholerae. *PLoS Pathog.* **9**,
582 e1003752 (2013).
583 12. Dong, T. G., Ho, B. T., Yoder-Himes, D. R. & Mekalanos, J. J. Identification of T6SS-
584 dependent effector and immunity proteins by Tn-seq in Vibrio cholerae. *Proc. Natl. Acad.*
585 *Sci.* **110**, 2623–2628 (2013).
586 13. Thomas, J., Watve, S. S., Ratcliff, W. C. & Hammer, B. K. Horizontal Gene Transfer of
587 Functional Type VI Killing Genes by Natural Transformation. *mBio* **8**, e00654-17 (2017).
588 14. Borgeaud, S., Metzger, L. C., Scrignari, T. & Blokesch, M. The type VI secretion system of
589 Vibrio cholerae fosters horizontal gene transfer. *Science* **347**, 63–67 (2015).
590 15. Kirchberger, P. C., Unterweger, D., Provenzano, D., Pukatzki, S. & Boucher, Y. Sequential
591 displacement of Type VI Secretion System effector genes leads to evolution of diverse
592 immunity gene arrays in Vibrio cholerae. *Sci. Rep.* **7**, 45133 (2017).
593 16. Hussain, N. A. S., Kirchberger, P. C., Case, R. J. & Boucher, Y. F. Modular Molecular
594 Weaponry Plays a Key Role in Competition Within an Environmental Vibrio cholerae
595 Population. *Front. Microbiol.* **12**, (2021).
596 17. Basler, M., Ho, B. T. & Mekalanos, J. J. Tit-for-tat: type VI secretion system counterattack
597 during bacterial cell-cell interactions. *Cell* **152**, 884–894 (2013).
598 18. Smith, W. P. J. *et al.* The evolution of tit-for-tat in bacteria via the type VI secretion system.
599 *Nat. Commun.* **11**, 5395 (2020).
600 19. LeRoux, M. *et al.* Kin cell lysis is a danger signal that activates antibacterial pathways of
601 Pseudomonas aeruginosa. *eLife* **4**, (2015).
602 20. Toska, J., Ho, B. T. & Mekalanos, J. J. Exopolysaccharide protects Vibrio cholerae from
603 exogenous attacks by the type 6 secretion system. *Proc. Natl. Acad. Sci.* **115**, 7997–8002
604 (2018).
605 21. Flaugnatti, N. *et al.* Human commensal gut Proteobacteria withstand type VI secretion
606 attacks through immunity protein-independent mechanisms. *Nat. Commun.* **12**, 5751 (2021).

607 22. McNally, L. *et al.* Killing by Type VI secretion drives genetic phase separation and correlates
608 with increased cooperation. *Nat. Commun.* **8**, 1–11 (2017).
609 23. Steinbach, G., Crisan, C., Ng, S. L., Hammer, B. K. & Yunker, P. J. Accumulation of dead
610 cells from contact killing facilitates coexistence in bacterial biofilms. *J. R. Soc. Interface* **17**,
611 20200486 (2020).
612 24. Crisan, C. V. *et al.* Glucose confers protection to Escherichia coli against contact killing by
613 Vibrio cholerae. *Sci. Rep.* **11**, 2935 (2021).
614 25. Hersch, S. J. *et al.* Envelope stress responses defend against type six secretion system
615 attacks independently of immunity proteins. *Nat. Microbiol.* **5**, 706–714 (2020).
616 26. Kamal, F. *et al.* Differential Cellular Response to Translocated Toxic Effectors and Physical
617 Penetration by the Type VI Secretion System. *Cell Rep.* **31**, (2020).
618 27. van Opijnen, T., Bodi, K. L. & Camilli, A. Tn-seq: high-throughput parallel sequencing for
619 fitness and genetic interaction studies in microorganisms. *Nat. Methods* **6**, 767–772 (2009).
620 28. Hersch, S. J., Sejuty, R. T., Manera, K. & Dong, T. G. High throughput identification of
621 genes conferring resistance or sensitivity to toxic effectors delivered by the type VI secretion
622 system. 2021.10.06.463450 Preprint at https://doi.org/10.1101/2021.10.06.463450 (2021).
623 29. Kawecki, T. J. *et al.* Experimental evolution. *Trends Ecol. Evol.* **27**, 547–560 (2012).
624 30. Levy, S. F. *et al.* Quantitative evolutionary dynamics using high-resolution lineage tracking.
625 *Nature* **519**, 181–186 (2015).
626 31. Melnyk, A. H., Wong, A. & Kassen, R. The fitness costs of antibiotic resistance mutations.
627 *Evol. Appl.* **8**, 273–283 (2015).
628 32. Miyata, S. T., Kitaoka, M., Brooks, T. M., McAuley, S. B. & Pukatzki, S. Vibrio cholerae
629 Requires the Type VI Secretion System Virulence Factor VasX To Kill Dictyostelium
630 discoideum. *Infect. Immun.* **79**, 2941–2949 (2011).
631 33. Altindis, E., Dong, T., Catalano, C. & Mekalanos, J. Secretome Analysis of Vibrio cholerae
632 Type VI Secretion System Reveals a New Effector-Immunity Pair. *mBio* **6**, e00075-15

633 (2015).
634 34. Brooks, T. M., Unterweger, D., Bachmann, V., Kostiuk, B. & Pukatzki, S. Lytic Activity of the
635 Vibrio cholerae Type VI Secretion Toxin VgrG-3 Is Inhibited by the Antitoxin TsaB *. *J. Biol.*
636 *Chem.* **288**, 7618–7625 (2013).
637 35. Luciano, D. J., Levenson-Palmer, R. & Belasco, J. G. Stresses that Raise Np4A Levels
638 Induce Protective Nucleoside Tetraphosphate Capping of Bacterial RNA. *Mol. Cell* **75**, 957-
639 966.e8 (2019).
640 36. Edwards, M. D. *et al.* Characterization of three novel mechanosensitive channel activities in
641 Escherichia coli. *Channels Austin Tex* **6**, 272–281 (2012).
642 37. Fivenson, E. M. & Bernhardt, T. G. An Essential Membrane Protein Modulates the
643 Proteolysis of LpxC to Control Lipopolysaccharide Synthesis in Escherichia coli. *mBio* **11**,
644 e00939-20 (2020).
645 38. Gabale, U., Peña Palomino, P. A., Kim, H., Chen, W. & Ressl, S. The essential inner
646 membrane protein YejM is a metalloenzyme. *Sci. Rep.* **10**, 17794 (2020).
647 39. Guest, R. L., Samé Guerra, D., Wissler, M., Grimm, J. & Silhavy, T. J. YejM Modulates
648 Activity of the YciM/FtsH Protease Complex To Prevent Lethal Accumulation of
649 Lipopolysaccharide. *mBio* **11**, e00598-20 (2020).
650 40. Amemiya, S. *et al.* The mechanosensitive channel YbdG from Escherichia coli has a role in
651 adaptation to osmotic up-shock. *J. Biol. Chem.* **294**, 12281–12292 (2019).
652 41. Crisan, C. V. *et al.* Analysis of Vibrio cholerae genomes identifies new type VI secretion
653 system gene clusters. *Genome Biol.* **20**, 163 (2019).
654 42. Bernardy, E. E., Turnsek, M. A., Wilson, S. K., Tarr, C. L. & Hammer, B. K. Diversity of
655 Clinical and Environmental Isolates of Vibrio cholerae in Natural Transformation and
656 Contact-Dependent Bacterial Killing Indicative of Type VI Secretion System Activity. *Appl.*
657 *Environ. Microbiol.* **82**, 2833–2842 (2016).
658 43. Ferenci, T. Trade-off Mechanisms Shaping the Diversity of Bacteria. *Trends Microbiol.* **24**,

659 209–223 (2016).
660 44. Lamrabet, O. *et al.* Plasticity of Promoter-Core Sequences Allows Bacteria to Compensate
661 for the Loss of a Key Global Regulatory Gene. *Mol. Biol. Evol.* **36**, 1121–1133 (2019).
662 45. Uppal, S., Maurya, S. R., Hire, R. S. & Jawali, N. Cyclic AMP receptor protein regulates
663 cspE, an early cold-inducible gene, in Escherichia coli. *J. Bacteriol.* **193**, 6142–6151 (2011).
664 46. Ji, X. *et al.* Alarmone Ap4A is elevated by aminoglycoside antibiotics and enhances their
665 bactericidal activity. *Proc. Natl. Acad. Sci. U. S. A.* **116**, 9578–9585 (2019).
666 47. Fan, J., Petersen, E. M., Hinds, T. R., Zheng, N. & Miller, S. I. Structure of an Inner
667 Membrane Protein Required for PhoPQ-Regulated Increases in Outer Membrane
668 Cardiolipin. *mBio* **11**, e03277-19 (2020).
669 48. Nurminen, M., Hirvas, L. & Vaara, M. The outer membrane of lipid A-deficient Escherichia
670 coli mutant LH530 has reduced levels of OmpF and leaks periplasmic enzymes. *Microbiol.*
671 *Read. Engl.* **143 (Pt 5)**, 1533–1537 (1997).
672 49. Dong, T. G. *et al.* Generation of reactive oxygen species by lethal attacks from competing
673 microbes. *Proc. Natl. Acad. Sci.* **112**, 2181–2186 (2015).
674 50. Myint, S. L. *et al.* Ecotin and LamB in Escherichia coli influence the susceptibility to Type VI
675 secretion-mediated interbacterial competition and killing by Vibrio cholerae. *Biochim.*
676 *Biophys. Acta BBA - Gen. Subj.* **1865**, 129912 (2021).
677 51. Lin, H.-H. *et al.* A High-Throughput Interbacterial Competition Screen Identifies ClpAP in
678 Enhancing Recipient Susceptibility to Type VI Secretion System-Mediated Attack by
679 Agrobacterium tumefaciens. *Front. Microbiol.* **10**, 3077 (2019).
680 52. Lee, H., Popodi, E., Tang, H. & Foster, P. L. Rate and molecular spectrum of spontaneous
681 mutations in the bacterium Escherichia coli as determined by whole-genome sequencing.
682 *Proc. Natl. Acad. Sci. U. S. A.* **109**, E2774-2783 (2012).
683 53. Blair, J. M. A., Webber, M. A., Baylay, A. J., Ogbolu, D. O. & Piddock, L. J. V. Molecular
684 mechanisms of antibiotic resistance. *Nat. Rev. Microbiol.* **13**, 42–51 (2015).

685 54. Schenk, M. F. & de Visser, J. A. G. Predicting the evolution of antibiotic resistance. *BMC*
686 *Biol.* **11**, 14 (2013).
687 55. Perron, G. G., Gonzalez, A. & Buckling, A. Source–sink dynamics shape the evolution of
688 antibiotic resistance and its pleiotropic fitness cost. *Proc. R. Soc. B Biol. Sci.* **274**, 2351–
689 2356 (2007).
690 56. Van den Bergh, B. *et al.* Frequency of antibiotic application drives rapid evolutionary
691 adaptation of Escherichia coli persistence. *Nat. Microbiol.* **1**, 1–7 (2016).
692 57. Herren, C. M. & Baym, M. Decreased thermal niche breadth as a trade-off of antibiotic
693 resistance. *ISME J.* **16**, 1843–1852 (2022).
694 58. Andersson, D. I., Patin, S. M., Nilsson, A. I. & Kugelberg, E. The Biological Cost of Antibiotic
695 Resistance. in *Enzyme-Mediated Resistance to Antibiotics* 339–348 (John Wiley & Sons,
696 Ltd, 2007). doi:10.1128/9781555815615.ch21.
697 59. Böttger, E. C., Springer, B., Pletschette, M. & Sander, P. Fitness of antibiotic-resistant
698 microorganisms and compensatory mutations. *Nat. Med.* **4**, 1343–1344 (1998).
699 60. Björkman, J., Nagaev, I., Berg, O. G., Hughes, D. & Andersson, D. I. Effects of environment
700 on compensatory mutations to ameliorate costs of antibiotic resistance. *Science* **287**, 1479–
701 1482 (2000).
702 61. Levin, B. R., Perrot, V. & Walker, N. Compensatory Mutations, Antibiotic Resistance and the
703 Population Genetics of Adaptive Evolution in Bacteria. *Genetics* **154**, 985–997 (2000).
704 62. van Hoek, A. *et al.* Acquired Antibiotic Resistance Genes: An Overview. *Front. Microbiol.* **2**,
705 (2011).
706 63. Fernández, L. & Hancock, R. E. W. Adaptive and Mutational Resistance: Role of Porins and
707 Efflux Pumps in Drug Resistance. *Clin. Microbiol. Rev.* **25**, 661–681 (2012).
708 64. Kim, S., Lieberman, T. D. & Kishony, R. Alternating antibiotic treatments constrain
709 evolutionary paths to multidrug resistance. *Proc. Natl. Acad. Sci.* **111**, 14494–14499 (2014).
710 65. Melnikov, S. V. *et al.* Exploiting evolutionary trade-offs for posttreatment management of

711 drug-resistant populations. *Proc. Natl. Acad. Sci.* **117**, 17924–17931 (2020).
712 66. Fischbach, M. A. Combination therapies for combating antimicrobial resistance. *Curr. Opin.*
713 *Microbiol.* **14**, 519–523 (2011).
714 67. Imamovic, L. & Sommer, M. O. A. Use of collateral sensitivity networks to design drug
715 cycling protocols that avoid resistance development. *Sci. Transl. Med.* **5**, 204ra132 (2013).
716 68. Madsen, J. S., Sørensen, S. J. & Burmølle, M. Bacterial social interactions and the
717 emergence of community-intrinsic properties. *Curr. Opin. Microbiol.* **42**, 104–109 (2018).
718 69. Li, Y.-H. & Tian, X.-L. Quorum Sensing and Bacterial Social Interactions in Biofilms:
719 Bacterial Cooperation and Competition. in *Stress and Environmental Regulation of Gene*
720 *Expression and Adaptation in Bacteria* 1195–1205 (John Wiley & Sons, Ltd, 2016).
721 doi:10.1002/9781119004813.ch116.
722 70. Silhavy, T. J., Berman, M. L. & Enquist, L. W. *Experiments with gene fusions*. (Cold Spring
723 Harbor Laboratory, 1984).
724 71. Thomason, L. C., Sawitzke, J. A., Li, X., Costantino, N. & Court, D. L. Recombineering:
725 Genetic Engineering in Bacteria Using Homologous Recombination. *Curr. Protoc. Mol. Biol.*
726 **106**, 1.16.1-1.16.39 (2014).
727 72. Baba, T. *et al.* Construction of Escherichia coli K-12 in-frame, single-gene knockout
728 mutants: the Keio collection. *Mol. Syst. Biol.* **2**, 2006.0008 (2006).
729 73. Jiang, W., Bikard, D., Cox, D., Zhang, F. & Marraffini, L. A. RNA-guided editing of bacterial
730 genomes using CRISPR-Cas systems. *Nat. Biotechnol.* **31**, 233–239 (2013).
731 74. McKenzie, G. J. & Craig, N. L. Fast, easy and efficient: site-specific insertion of transgenes
732 into enterobacterial chromosomes using Tn7 without need for selection of the insertion
733 event. *BMC Microbiol.* **6**, 39 (2006).
734 75. Hart, E. M., Gupta, M., Wühr, M. & Silhavy, T. J. The Synthetic Phenotype of ΔbamB
735 ΔbamE Double Mutants Results from a Lethal Jamming of the Bam Complex by the
736 Lipoprotein RcsF. *mBio* **10**, e00662-19 (2019).

737 76. Skorupski, K. & Taylor, R. K. Positive selection vectors for allelic exchange. *Gene* **169**, 47–
738 52 (1996).
739 77. Watve, S. S., Thomas, J. & Hammer, B. K. CytR Is a Global Positive Regulator of
740 Competence, Type VI Secretion, and Chitinases in Vibrio cholerae. *PLOS ONE* **10**,
741 e0138834 (2015).
742 78. Chen, S., Zhou, Y., Chen, Y. & Gu, J. fastp: an ultra-fast all-in-one FASTQ preprocessor.
743 *Bioinformatics* **34**, i884–i890 (2018).
744 79. Deatherage, D. E. & Barrick, J. E. Identification of mutations in laboratory-evolved microbes
745 from next-generation sequencing data using breseq. *Methods Mol. Biol. Clifton NJ* **1151**,
746 165–188 (2014).
747 80. Langmead, B. & Salzberg, S. L. Fast gapped-read alignment with Bowtie 2. *Nat. Methods* **9**,
748 357–359 (2012).
749 81. NCBI Resource Coordinators. Database resources of the National Center for Biotechnology
750 Information. *Nucleic Acids Res.* **44**, D7-19 (2016).